Minicolumnar pathology in autism

Manuel F. Casanova, MD; Daniel P. Buxhoeveden, PhD; Andrew E. Switala; and Emil Roy, PhD

Abstract—*Objective:* To determine whether differences exist in the configuration of minicolumns between the brains of autistic and control patients. *Background:* Autism is a severe and pervasive developmental disturbance of childhood characterized by disturbances in both social interactions and communication, as well as stereotyped patterns of interests, activities, and behaviors. Postmortem neuropathologic studies remain inconclusive. *Methods:* The authors used a computerized imaging program to measure details of cell column morphologic features in area 9 of the prefrontal cortex and areas 21 and posterior 22 (Tpt) within the temporal lobe of nine brains of autistic patients and controls. *Results:* The authors found significant differences between brains of autistic patients and controls in the number of minicolumns, in the horizontal spacing that separates cell columns**,** and in their internal structure, that is, relative dispersion of cells. Specifically, cell columns in brains of autistic patients were more numerous, smaller, and less compact in their cellular configuration with reduced neuropil space in the periphery. *Conclusions:* In autism, there are minicolumnar abnormalities in the frontal and temporal lobes of the brain.

NEUROLOGY 2002;58:428–432

Existing neuropathologic studies of autism provide for subtle if not mixed results. The subjective nature of the methodology and small case series may partially explain the disparate findings. Alternatively, attempts based on classic neuropathologic methods and its emphasis on cellular changes would necessarily prove unrewarding if the underlying disturbance is one of circuitry. Given the importance of neocortical cellular organization and circuitry during development, we focused on the single radial column or cell minicolumn. The minicolumn is a basic functional unit of the brain that organizes neurons in cortical space.[1-4] Thus, changes based on circuitry or spatial morphologic features may affect this fundamental unit of cortical structure.

Materials and methods. Material for this study included nine autistic and four control subjects from the Autism Research Foundation. Drs. M. Bauman and T. Kemper provided for diagnosis, tissue collection and processing. Specimens are readily available at Boston Medical Center. Five additional controls were taken from the Yakovlev–Haleem Collection, National Museum of Health and Medicine, Armed Forces Institute of Pathology, Washington, D.C. Mean age was 12 years for autistic cases and 15 for controls. Diagnostic and postmortem information on the autistic cases has been reported elsewhere (table).[5-14] The brains had been celloidin imbedded and cut into 35-μm serial sections and Nissl stained. Adjacent slides were stained with the Loyez technique.

We obtained digitized images of lamina III in each of three cortical areas: 9, posterior 22, and the middle temporal gyrus (area 21). Some areas were unavailable for several of the case subjects and were considered as an unbalanced design.

Minicolumns. In a minicolumn, a core line of neurons ascends vertically between layers VI and II. Most of the cells aggregate in a linear fashion; a cell-poor area, usually denoted as the peripheral neuropil space, surrounds both sides. This area, which is noticeable in a cell body stain, is rich in unmyelinated axon fibers, dendritic arborizations, and synapses.[15] The core area of a column and its immediate surroundings appear to contain most of the neurons, apical dendrites, cortical efferents, and corticocortical fibers, as well as unmyelinated axons and synapses.[16] Myelinated axon bundles presumably are cortical efferents originating in pyramidal cells in layers II and III. These bundles descend toward the white matter, lying within or adjacent to the cellular core of a column. Apical dendrites originating in layer V pyramidal cells ascend in bundles through or adjacent to the cell column core.[17] The edges of the column core contain vertical fiber bundles of GABAergic interneurons. These bundles—especially marked in lamina III—are a source of lateral inhibition that is believed to delineate individual minicolumns from their neighbors.[2,3,18]

Cortical areas. Area 21 is located primarily within the middle temporal gyrus on the lateral surface of the brain hemisphere. It lies bordered by areas 20 (ventral), 22 (dorsal), 37 (caudal), and 38 (rostral). The surrounding areas are paralimbic[19,20] and auditory parasensory.[21] Area 21 is considered visual parasensory association cortex. Myeloarchitectonic studies have shown a scarcity of myelinated fibers. At higher magnification, area 21 has a well-defined layer IIIb, which lies rectilinearly opposed to layer IV.

Area 9 lies in the superior and middle frontal gyrus. Researchers have found[19,22] that it is located in the middle third of the superior frontal gyrus covering both its dorsolateral and dorsomedial surfaces. Microscopically, area 9 has a poorly defined lamina IV.[23]

Within Brodmann area 22, we focused on the tem-

From Medical College of Georgia (Dr. Casanova), Augusta; Department of Anthropology (Dr. Buxhoeveden), University of South Carolina, Columbia; and Downtown Veterans Administration Medical Center (Drs. Casanova and Roy, and A. Switala), Augusta, GA.

Supported by grants from the Theodore and Vada Stanley Foundation and the VA Merit Review Board.

Received November 27, 2000. Accepted in final form October 11, 2001.

Address correspondence and reprint requests to Dr. Manuel F. Casanova, Downtown VA Medical Center, 26 Psychiatry Service, 3B-121, Augusta, GA 30910; e-mail: casanova@np2.mcg.edu

Table *Summary data on autistic patients*

Brain	Age	MR	Seizures	ADI	Cause of death
BCH-AUT-84	10	Yes	Yes	Yes	Peritonitis
BCH-AUT-85	9	*	Yes	Yes	*
BCH-AUT-87	28	Yes	No	Yes	Cardiac arrest (diabetic)
BCH-AUT-87-2	22	Yes	Yes	*	Drowned
BCH-AUT-87-3	12	No	No	Yes	Bone tumor metastasized to lung
BCH-AUT-88	9	Yes	*	No	*
BCH-AUT-88-2	7	Yes	No	Yes	Drowned
BCH-AUT-89-3	5	Yes	Yes	Yes	Found dead in bed
BCH-AUT-91	6	Yes	Yes	Yes	Asphyxiation (secondary to drowning)

* Information missing from patients' records.

ADI = autism diagnostic interview; MR = mental retardation.

poroparietal auditory area (Tpt), which covers the lateral aspects of the superior temporal gyrus (STG) posterior to the caudal parabelt cortex up to the bank of the superior temporal sulcus, as well as the most posterior portions of the superior surface of the supratemporal plane (the planum temporale).[21,24-31] Because no sulcal demarcation exists for Tpt, it must be discerned microscopically from its general location on the STG. Tpt is located in the posterior regions of the STG: it appears immediately behind and lateral to the parabelt region labeled as caudal auditory parabelt (CP).[26-28] It also appears on the most posterior portion of the superior surface of the supratemporal plane. Qualitatively, adult Tpt is characterized by having all six cortical layers well formed, an undulating border between layers III and IV, an indistinct border between IV and V, and an "organ-pipe" organization (distinct curvilinear columns of neurons arising in an irregular fashion from the white matter) in layer VI.[25,31]

Procedures. Our method is a modification of an earlier version described elsewhere.[32] A region of interest (ROI) must be isolated and transferred to the computer imaging system. The ROI is obtained from a microscopic field of view at a chosen magnification. Magnifications of 100× are chosen to resolve both individual perikarya and the complete laminar depth. Usually, the ROI consists of the entire field of view as seen in the photomicrograph; however, the field is cropped as needed to exclude tissue distortions and superfluous features such as vessels.

The first stage of the column detection routine divides a region of interest into overlapping horizontal strips. Cell concentration ν is defined for each strip by

$$\nu(x) \equiv \sum_i e^{-8(x-x_i)^2/d^2}$$

the sum being taken over all cells in that strip. The characteristic scale d is the width of a box that, placed at random in the field, would enclose one cell on average. The relative maxima and minima of ν mark the locations of the centers of aggregation of cell columns and the space between them. Notice that the full width of the Gaussian in the definition of ν is such that cells within less than $\frac{1}{2}d$ of each other contribute to the same relative maximum of ν and are not resolved into distinct columns. For the primary contribution to ν come from a region containing, on average, one cell, the height of the horizontal strips is approximately $2d$. Minicolumns are defined by the method as vertical clusters of large neurons delimited on either side by cell-sparse areas. Imaginary lines through the sparse areas partition a field into polygonal regions (figure 1). We refer to such a polygon together with the totality of small and large neurons contained within it as a minicolumn segment, from which we obtain several descriptive statistics.

For this study, we report on five measures: columnar width (CW), peripheral neuropil space (NS), interneuronal distance (MCS), compactness (RDR), and gray level index (GLI). CW describes the diameter of a single minicolumn, or equivalently, the center-to-center distance between adjacent minicolumns. NS is the width of the cell-poor space on both sides of the minicolumn, found by subtracting the width of the column core from the CW. The column core is defined as that part of the column that contains 90% of the cell bodies. Up to 10% of the cells in the column may lie in the region designated as peripheral neuropil space so that the measurement of NS is insensitive to "outlier" points. MCS is the mean distance between nearby neurons within a column. The compactness parameter RDR is the ratio of second moments of the distribution of cells (the ratio of the greater to the lesser) divided by the ratio of second moments of the entire minicolumn, including its empty space.

Because ours is not a cell counting method, we prefer to account for overall cell density by measuring the area fraction occupied by Nissl-stained segments, called the GLI.[33] Before column detection, the GLI is computed from the original image by thresholding. The total area of Nissl-stained objects, that is, the number of pixels below the threshold, is divided by the image area to yield the GLI. Whereas this measurement does not provide us with cell numbers, it estimates the amount of space within the minicolumns occupied by cell somas.

Results. A multivariate analysis of variance was performed with diagnosis, that is, normal or autistic, hemisphere, and cortical area as a fixed factor and CW, NS, MCS, RDR, and GLI as the dependent variables. Age was included as a covariate. Preliminary testing included the source of material (Yakovlev or Bauman-Kemper) as a fixed factor to test for possible differences between control brains from the two collections (none were found). The

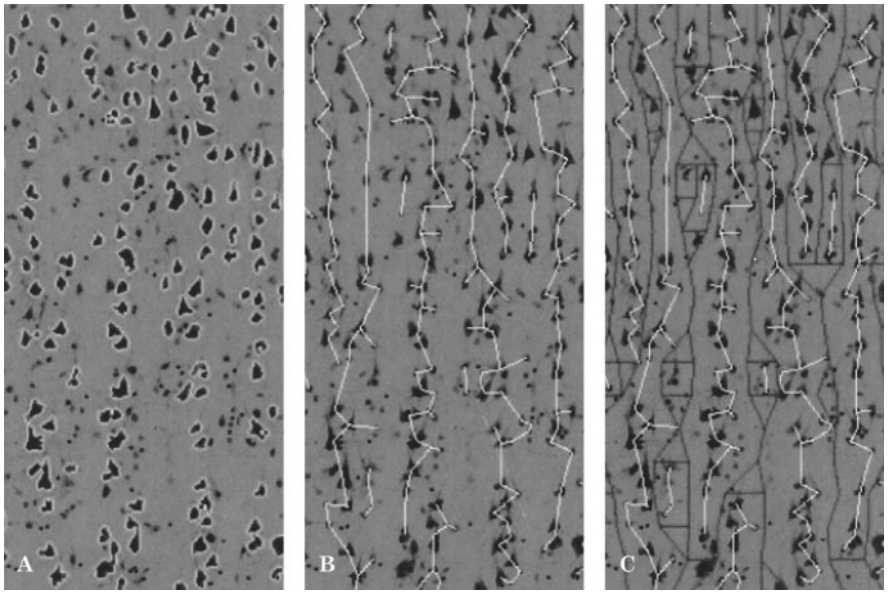

Figure 1. (A) Neurons used by the column detection routine to identify areas of high cell concentration are outlined in white. Image taken in layer III of temporoparietal auditory area cortex in normal brain (original magnification ×100). (B) White lines depict the Euclidean minimum spanning trees of the cell column segments, used by the analysis routine to describe minicolumn structure. (C) Black lines depict the boundaries of the areas of high cell concentration used by the analysis routine to compute column width and peripheral neuropil space.

overall multivariate test, using the Wilks Λ, revealed differences between autistic patients and controls with $p = 0.002$. The area * diagnosis interaction term was $p = 0.388$. Minicolumns were found to be narrower in autism with a mean CW of 46.8 vs 52.8 μm in the normal brain ($p = 0.034$). NS was reduced in the mean: 22.8 μm in controls compared with 18.7 μm in autism ($p = 0.007$), as was RDR, 1.37 in controls and 1.19 in autism ($p = 0.001$). Differences in MCS and GLI were on the order of 1% of their values in controls: 25.8 μm and 19.4%.

Differences between populations can be visualized with the aid of principal component analysis of the parameters CW, MCS, NS, and RDR. Because the parameters have different scales of measurement, principal components were extracted from the sample correlation matrix rather than the covariance matrix. The first two are: $C_1 = 0.566 \cdot CW'; + 0.390 \cdot MCS'; + 0.561 \cdot NS'; + 0.475 \cdot RDR';$ and $C_2 = 0.059 \cdot CW'; - 0.826 \cdot MCS'; + 0.041 \cdot NS'; + 0.560 \cdot RDR';$ accounting for 91% of the variation in the data. Primes signify that variables are standardized to zero mean and unit variance. C_1 seems to measure overall column size, taking into account the positive correlations of CW with the other three parameters, whereas C_2, dependent mostly on MCS and RDR, is a measure of cell concentration (figure 2).

Four of the nine autistic cases were macroencephalic, with brain weights more than two standard deviations above the means for their corresponding ages.[34] One of these, however, showed a generalized edema. Brain weight was unavailable for most of the controls and thus could not be factored into the analysis. Fresh weights were available for one normal and all brains of autistic patients, however. Analysis of these cases suggests that brain weight does not correlate closely with CW ($r = 0.04$, $p = 0.812$), MCS ($r = -0.03$, $p = 0.850$), NS ($r = 0.03$, $p = 0.862$), RDR ($r = -0.19$, $p = 0.303$), or GLI ($r = -0.18$, $p = 0.325$). The missing weight data, therefore, are not expected to bias the results.

Discussion. Our results indicate that the cell minicolumns of autistic patients are reduced in width as compared with subjects. Specifically, cell columns in brains of autistic patients are significantly smaller and less compact in their configuration (i.e., cells are more dispersed), with less neuropil space in their periphery. The abnormality is found in all three regions of interest examined, that is, area 9 of the prefrontal cortex, and areas 21 and 22 (Tpt) of the temporal lobe. Also, the results indicate that the overall gray level index does not differ between groups.

The gray level index in this study used a scale of several hundred microns and is a measure of cell density. Elsewhere,[35] we report gray level index abnormalities when using the same patient population. The latter results were obtained using a method[36] that describes inhomogeneities on a scale of 10 μm.

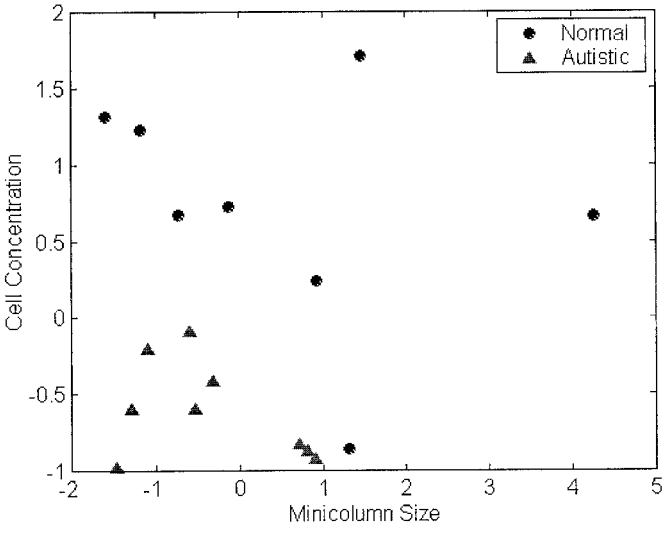

Figure 2. The first two principal components, which represent minicolumn size and cell concentration, clearly distinguish autistic from control cases. (Data shown for temporoparietal auditory area.)

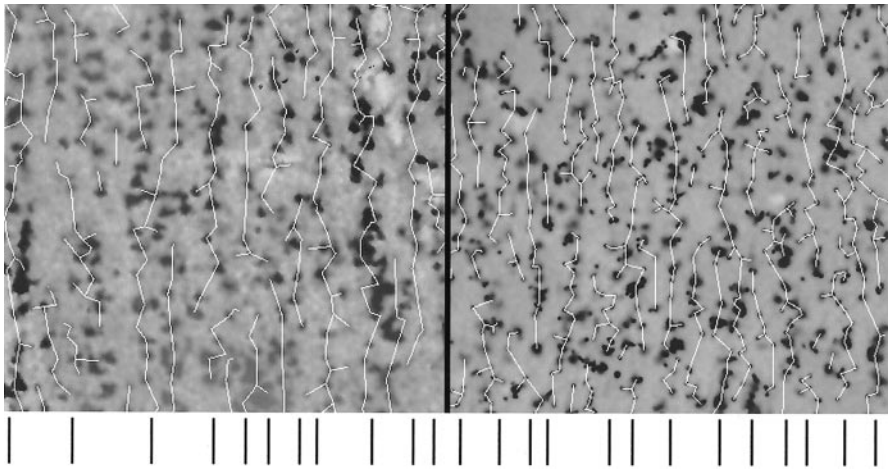

Figure 3. Microscopic fields (original magnification ×100) of layer III of temporoparietal auditory area from the brain of an autistic patient (right) and an age-matched control (left). The superimposed Euclidean minimum spanning tree indicates the cell core of the minicolumn. Lines at the bottom of each figure define the boundaries of each minicolumn, that is, 10 in the control brain and 12 in the brain of the autistic patient. Computerized analysis of our series reveals greater neuronal dispersion and normal cell density in the brains of autistic patients.

Taken together, the gray level indices suggest a distinction in the small-scale distribution of cells without a corresponding difference in cell density. It therefore makes sense that individual cells in the smaller minicolumns in brains of autistic patients are more dispersed as reflected by their relative dispersion ratio (i.e., RDR parameter, which represents cell compactness).

All of the measurements in our sample were provided per microscopic field. This means that the brain of the autistic patient has more minicolumns, albeit of reduced size, per longitudinal expanse of cortex (figure 3). This novel cytoarchitectural arrangement may originate during the neurogenesis of the cell minicolumn. The evolution of the mammalian brain emphasizes expansion of cortical surface rather than thickness. This is evident by the almost 1,000-fold increase in cortical surface versus only a twofold increase in cortical width.[37] Investigators[37] postulate that the observed enlargement in cortical surface stems from an increase in number of ontogenetic cell columns. In this model, new patterns of connections brought about by an increased number of minicolumns would be established if they were "validated" by natural selection. Additional studies are needed to determine whether these supernumerary columns are caused by a mutation in the regulatory genes that control the timing and ratio of symmetric and asymmetric cell divisions in the proliferative zone.

Evolution has kept column (mini and macro) size essentially constant while increasing total cortical surface area, which, in larger brains, has resulted in more columns per brain and thus more processing units and increased complexity.[20,38] During this slow process, selection pressures ensured that the addition of new cell columns would benefit the organisms or at least not prove maladaptive. In autism, a significant increase in processing units may occur, an acute event not subject to normal selection pressures.

If thalamic terminations remain the same in autism (uncertain at this time) and minicolumns are smaller, then more minicolumns will be innervated per thalamic afferent terminal than in the normal brain. The failure to assimilate extra processing units by the connectivity patterns of the brain may result in cortical "noise," that is, additional units of activity that overtax the system.

Among several conceptual classifications, autism has been considered a disorder of the arousal-modulating systems of the brain.[39] According to this theory, autistic individuals experience a chronic state of overarousal and exhibit abnormal behaviors to diminish this arousal. The arousal theory is of some interest because it is consistent with a reduction of inhibitory interneuronal activity. It is known that the cortex contains inhibitory double bouquet cells that define minicolumnar organization for the brain,[40] or what one researcher calls a "strong vertically directed stream of inhibition".[1] The lateral inhibition caused by the GABAergic neurons helps to ensure individual minicolumn discreteness and during development, to impel adjacent minicolumns into establishing connections with functionally dissimilar sets of thalamic neurons.[2,3] A lack of these lateral inhibitors would grossly alter the connective patterns between thalamic input and column, tending toward convergence. The result would affect the ability to discriminate between competing types of sensory information.

Acknowledgment

The authors thank the Autism Research Foundation, Dr. Margaret L. Bauman (Department of Neurology, Harvard Medical School, Boston, MA), and Dr. Thomas S. Kemper (Department of Pathology, Anatomy and Neurobiology, and Neurology, Boston University School of Medicine, Boston, MA) for helpful advice and for providing facilities for this study.

References

1. Mountcastle VB. The columnar organization of the neocortex. Brain 1997;120:701–722.
2. Favorov OV, Kelly G. Minicolumnar organization within somatosensory cortical segregates. I: development of afferent connections. Cereb Cortex 1994a;4:408–427.
3. Favorov OV, Kelly G. Minicolumnar organization within somatosensory cortical segregates. II: emergent functional properties. Cereb Cortex 1994b;4:428–442.

4. Tommerdahl M, Favorov O, Whitsel BL, Nakhle B, Gonchar YA. Minicolumnar activation patterns in cat and monkey S1 cortex. Cereb Cortex 1993;3(5):399–411.
5. Bauman ML. Microscopic neuroanatomic abnormalities in autism. Pediatrics 1991;87:791–796.
6. Bauman ML, Kemper TL. The brain in infantile autism: a histoanatomic case report. Neurol. 1984;34(suppl 1):275.
7. Bauman M, Kemper TL. Histoanatomic observations of the brain in early infantile autism. Neurology 1985;35:866–874.
8. Bauman ML, Kemper TL. Developmental cerebellar abnormalities: a consistent finding in early infantile autism. Neurology 1986;36(suppl 1):190.
9. Bauman ML, Kemper TL. Limbic involvement in a second case of early infantile autism. Neurology 1987;37(suppl 1):147.
10. Bauman ML, Kemper TL. Limbic and cerebellar abnormalities: consistent findings in infantile autism. J Neuropathol Exp Neurol 1988;47:369.
11. Bauman ML, Kemper TL. Abnormal cerebellar circuitry in autism? Neurology 1989;39(suppl 1):186.
12. Bauman ML, Kemper TL. Neuroanatomic observations of the brain in autism. In: Bauman ML, Kemper TL, eds. The neurobiology of autism. Baltimore: The Johns Hopkins University Press, 1996:119–145.
13. Kemper TL, Bauman M. Neuropathology of infantile autism. J Neuropathol Exp Neurol 1998;57:645–652.
14. Raymond GV, Bauman ML, Kemper TL. Hippocampus in autism: a Golgi analysis. Acta Neuropathol 1996;91:117–119.
15. Seldon HL. Structure of human auditory cortex. I: cytoarchitectonics and dendritic distributions. Brain Res 1981;229:277–294.
16. Peters A, Sethares C. Myelinated axons and the pyramidal cell modules in monkey primary visual cortex. J Comp Neurol 1996;365:232–55.
17. Peters A, Walsh TM. A study of the organization of apical dendrites in the somatic sensory cortex of the rat. J Comp Neurol 1972;144:253–268.
18. DeFelipe J, Hendry S, Hashikawa T, Molinari M, Jones EG. A microcolumnar structure of monkey cerebral cortex revealed by immunocytochemical studies of double bouquet cell axons. Neuroscience 1990;37:655–673.
19. Rajkowska G, Goldman-Rakic PS. Cytoarchitectonic definition of prefrontal areas in the normal human cortex. II: variability in locations of areas 9 and 46 and relationship to the Talairach coordinate system. Cereb Cortex 1995;5:323–337.
20. Rakic P, Suner I, Williams RW. A novel cytoarchitectonic area induced experimentally within the primate visual cortex. Proc Natl Acad Sci USA 1991;88:2083–2087.
21. Galaburda AM, LeMay M, Kemper TL, et al. Right–left asymmetries in the brain: structural differences between the hemispheres may underlie cerebral dominance. Science 1978;199:852–856.
22. Rajkowska G, Goldman-Rakic PS. Cytoarchitectonic definition of prefrontal areas in the normal human cortex. I: Remapping of areas 9 and 46 using quantitative criteria. Cereb Cortex 1995;5:307–322.
23. Petrides M, Pandya DN. Dorsolateral prefrontal cortex: comparative cytoarchitectonic analysis in the human and macaque brain and corticocortical connection patterns. Eur J Neurosci 1999;II:11–36.
24. Galaburda AM, Sanides F, Geschwind N. Human brain: cytoarchitectonic left–right asymmetries in the temporal speech region. Arch Neurol 1978;35:812–817.
25. Galaburda AM, Sanides F. Cytoarchitectonic organization of the human auditory cortex. J Comp Neurol 1980;190:597–610.
26. Hackett TA, Stepniewska I, Kaas JH. Subdivisions of auditory cortex and ipsilateral cortical connections of the parabelt auditory cortex in macaque monkeys. J Comp Neurol 1998;394:475–495.
27. Hackett TA, Stepniewska I, Kaas JH. Thalamocortical connections of the parabelt auditory cortex in macaque monkeys. J Comp Neurol 1998b;400:271–286.
28. Hackett TA, Stepniewska I, Kaas JH. Prefrontal connections of the parabelt auditory cortex in macaque monkeys. Brain Res 1999;817:45–58.
29. Romanski LM, Bates JF, Goldman-Rakic PS. Auditory belt and parabelt projections to the prefrontal cortex in the rhesus monkey. J Comp Neurol 1999;403:141–157.
30. Witelson SF, Glezer II, Kigar DL. Women have greater density of neurons in posterior temporal cortex. J Neurosci 1995;15:3418–3428.
31. Galaburda AM, Pandya DN. The intrinsic, architectonic and connectional organization of the superior temporal region of the rhesus monkey. J Comp Neurol 1983;221:169–184.
32. Buxhoeveden DP, Switala AE, Roy E, Casanova MF. Quantitative analysis of cell columns in the cerebral cortex. J Neurosci Methods 2000;97:7–17.
33. Wree A, Schleicher A, Zilles K. Estimation of volume fractions in nervous tissue with an image analyzer. J Neurosci Methods 1982;6:29–43.
34. Dekaban AS, Sadowsky D. Changes in brain weights during the span of human life: relation of brain weights to body heights and body weights. Ann Neurol 1978;4:345–356.
35. Casanova MF, Buxhoeveden D, Switala A, Roy E. Gray level index abnormalities in the brains of autistic patients. Proceedings Summary of the American Psychiatric Association Annual Meeting, 2001;NR 726.
36. Schlaug G, Schleicher A, Zilles K. Quantitative analysis of the columnar arrangement of neurons in the human cingulate cortex. J Comp Neurol 1995;351:441–452.
37. Rakic P. One small step for the cell, a giant leap for mankind: a hypothesis of neocortical expansion during evolution. Trends Neurosci 1995;18:383–388. Review.
38. Bugbee NM, Goldman-Rakic PS. Columnar organization of corticocortical projections in squirrel and rhesus monkeys: similarity of column width in species differing in cortical volume. J Comp Neurol 1983;220:355–364.
39. Hutt SJ, Hutt C, Lee D, Ounsted C. A behavioral and electroencephalographic study of autistic children. J Psychiatr Res 1964;181–187:
40. DeFelipe J, Hendry S, Hashikawa T, Molinari M, Jones EG. A microcolumnar structure of monkey cerebral cortex revealed by immunocytochemical studies of double bouquet cell axons. Neuroscience 1990;37:655–673.